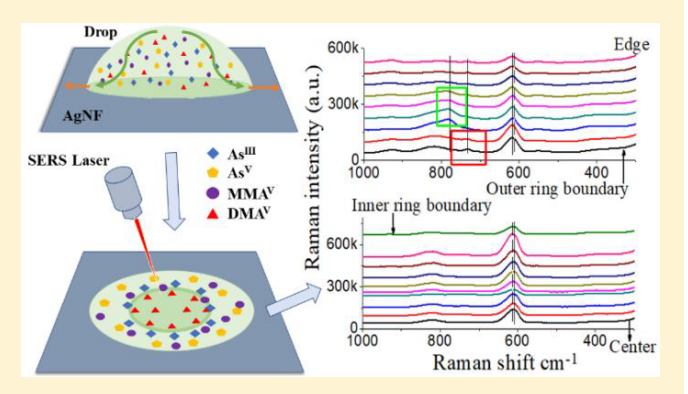


# Arsenic Speciation on Silver Nanofilms by Surface-Enhanced Raman Spectroscopy

Mingwei Yang, †,‡ Valery Liamtsau, †,‡ Changjun Fan, † Kelli L. Sylvers,  $^{\$,\parallel}$  Anthony J. McGoron,  $^{\perp}$  Guangliang Liu,  $^{\dagger,\nabla_{\textcircled{\tiny{0}}}}$  Fengfu Fu,  $^{\diamondsuit_{\textcircled{\tiny{0}}}}$  and Yong Cai $^{*,\dagger,\nabla_{\textcircled{\tiny{0}}}}$ 

Supporting Information

ABSTRACT: Surface-enhanced Raman spectroscopy (SERS), as a nondestructive and fast detection technique, is a promising alternative approach for arsenic detection, particularly for in situ applications. SERS-based speciation analysis according to the fingerprint SERS signals of different arsenicals has the potential to provide a superior technique in species preservation over the conventional chromatographic separation methods, albeit with some difficulties due to the similarity in SERS patterns. In this study, we explored a novel SERS method for arsenic speciation by using the separation potential of the coffee ring effect on negatively charged silver nanofilms (AgNFs). Four arsenic species, including arsenite (As<sup>III</sup>), arsenate (As<sup>V</sup>), monomethylarsonic acid (MMA<sup>V</sup>), and



dimethylarsinic acid (DMAV), were measured for fingerprint SERS signals in solution and on the films. Significant enhancement of SERS signals on the dried coffee ring stains by the AgNFs were observed except for As<sup>III</sup>, and more importantly, arsenicals migrated varying distances during coffee ring development, promoting better speciation. Sodium dodecyl sulfate was then introduced into the droplet to reduce the droplet surface tension, facilitating the migration of solution into the peripheral region. Under the combined interactions of arsenicals with the AgNFs, solvent, and surfactant, enhanced separation between arsenicals was observed as a result of the formation of two concentric rings. Combining the SERS fingerprint signals and physical separation of arsenicals on the surface, arsenic speciation was achieved using the AgNFs substrate-based SERS technology, demonstrating the potential of the coffee ring effect for rapid separation and analysis of small molecules by SERS.

#### ■ INTRODUCTION

Speciation analysis of toxic metals and metalloids is often performed by separation of different species followed by detection. For arsenic speciation, the conventional method is the combination of chromatographic separation with spectrometric detection techniques. The popular separation techniques include high-performance liquid chromatography (HPLC), i ion chromatography (IC), 2,3 and capillary electrophoresis (CE),4 and the detection techniques include mass spectrometry,<sup>5</sup> UV-vis absorption,<sup>6</sup> and hydride generation coupled with atomic fluorescence or absorption spectrometry (HG-AFS or HG-AAS). However, these popular analytical techniques have great limitations for arsenic speciation in biological matrices, since it is difficult to maintain the integrity of the arsenic species due to species transformation during sample preparation, separation, or detection. 1,8-10

Surface-enhanced Raman spectroscopy (SERS) has been recognized as an advanced analytical technique for decades, owing to its unique advantages, e.g., fast and noninvasive detection and single-molecule sensitivity. The employment of SERS in arsenic detection has been reported recently, mainly with metallic nanoparticles 11-13 and metallic nanofilms 14-19 as substrates, while indirect detection methods use aptamers to boost the arsenic molecules selectivity. 20,21 A review article regarding the recent advancements in arsenic detection based on SERS is available.<sup>22</sup> Though in theory SERS could be used to carry out arsenic speciation using the unique fingerprint spectra of target compounds without chromatographic

Received: February 24, 2019 Accepted: June 4, 2019 Published: June 4, 2019



 $<sup>^\</sup>dagger$ Department of Chemistry and Biochemistry and  $^\nabla$ Southeast Environmental Research Center, Florida International University, 11200 Southwest Eighth Street, Miami, Florida 33199, United States

Department of Chemistry and Physical Sciences, The College of St. Scholastica, 1200 Kenwood Avenue, Duluth, Minnesota 55811, United States

<sup>&</sup>lt;sup>⊥</sup>Biomedical Engineering Department, Florida International University, 10555 West Flagler Street, Miami, Florida 33174, United States

<sup>♦</sup> College of Chemistry, Fuzhou University, Fuzhou, Fujian 350116, China

separation, difficulties were often encountered for the simultaneous measurement due to spectrum overlap. For example, two inorganic arsenic compounds (arsenite (As<sup>III</sup>), arsenate (As<sup>V</sup>)) were able to be measured using SERS without significant spectrum overlapping. However, two structurally similar organic arsenicals, monomethylarsonic acid (MMA<sup>V</sup>) and dimethylarsinic acid (DMA<sup>V</sup>), in silver colloidal suspensions could not be distinguished by SERS due to their similar Raman spectra, as reported in our recent work. Therefore, when using SERS for speciation analysis, it is ideal to develop a separation method that minimizes the transformation of arsenic species and can be coupled to SERS, where SERS fingerprint signals and physical separation of arsenicals would provide a combined power for arsenic speciation.

The coffee ring effect refers to the occurrence of the ringshaped stain left on a solid surface when a coffee drop is dried on the solid surface.<sup>25</sup> With the evaporation of liquid over the liquid drop surface, liquid from the center region would migrate toward the edge to replenish the loss of liquid, and the movement of liquid from the center to the edge is driven by the capillary flow.<sup>25</sup> The coffee ring effect has been coupled with SERS measurements for the simplicity of operation to concentrate analytes toward the coffee ring region and to boost the detection sensitivity simultaneously. 26,27° The coffee ring effect showed potential to separate nano/microparticles, because different size particles have different accessibilities toward the contact line during the evaporation process.<sup>28,29</sup> The results of these previous studies showed the potential application of using the coffee ring as a simple platform for chemical separation/speciation.

Despite the absence of directly using the coffee ring effect for separation of small molecules, thin layer chromatography (TLC), a technique with certain resemblance to coffee ring development, has been coupled to SERS for separation and detection of various analytes. Recently, the TLC-SERS technique had been applied for facile measurement of environmental pollutants, 30 drugs, 31,32 and dyes. 33 The target analytes were usually eluted with a mobile phase and separated on a commercially available TLC plate. The analytes could be then detected by SERS after coating with silver/gold nanoparticles colloids serving as SERS substrates. Compared to TLC, separation of analytes driven by the coffee ring effect without consumption of mobile solution offers shorter development times and would be more suitable for in situ analysis. It is, therefore, of our interest to use the coffee ring effect for separation of small molecules based on different interactions of the analytes with the surface and solvent for being coupled to SERS for speciation analysis.

In this study, we explored a novel SERS method for arsenic speciation by combining the separation potential of the coffee ring effect on negatively charged silver nanofilms (AgNFs) and the Raman signal enhancement on AgNFs through analysis of four common arsenic species, arsenite (As<sup>III</sup>), arsenate (As<sup>V</sup>), monomethylarsonic acid (MMA<sup>V</sup>), and dimethylarsinic acid (DMA<sup>V</sup>). Surfactants were introduced into the droplet in order to reduce the droplet surface tension and facilitate migration of solution into the peripheral region of the droplet for enhanced separation. <sup>34–36</sup> Under the combined interactions of arsenicals with the AgNFs, solvent, and surfactant, arsenicals traveled different distances away from the drop center and were partially separated on the AgNFs after drying the solution drop. Combining the SERS fingerprint signals and physical

separation of arsenicals on the surface, arsenic speciation was achieved using the AgNFs substrate-based SERS technology.

#### **EXPERIMENTAL METHODS**

**Caution:** The arsenic species included in this study are toxic and could be potential human carcinogens, and they should be handled with care.

Materials and Chemicals. Sodium metaarsenite, 98% (As<sup>III</sup>), sodium arsenate dibasic, 99% (As<sup>V</sup>), and cacodylic acid sodium salt, 98% (DMAV), were obtained from Sigma-Aldrich (St. Louis, MO). Monosodium acid methane arsonate, 99.5% (MMA<sup>V</sup>), was obtained from Chem Service, USA. Silver nitrate (99.99%) was purchased from STREM chemicals (Newburyport, MA). Sodium citrate dihydrate (Granular certified), NaOH, HCl, K2HPO4, and KH2PO4 were certified A.C.S grade or higher and purchased from Fisher Scientific Inc. The phosphate buffer was prepared by mixing an equal volume of 0.2 mol L<sup>-1</sup> of K<sub>2</sub>HPO<sub>4</sub> and KH<sub>2</sub>PO<sub>4</sub>. Sodium dodecyl sulfate (SDS, 99.0%) and (3-aminopropyl) trimethoxysilane (APTMS) were purchased from Sigma-Aldrich (St. Louis, MO). All solutions were prepared in deionized water (DI water) (18.2 M $\Omega$ , Barnstead Nanopure Diamond) unless with specific indication. All arsenic stock solutions were prepared in DI water at  $13.3 \times 10^{-3}$  mol L<sup>-1</sup> (1000 ppm as arsenic atomic concentration). Glass microscope slides, purchased from Fisher Scientific (Pittsburgh, PA), were cut into  $1 \times 1$  cm<sup>2</sup> pieces as glass substrates. Small size weighing boats were purchased from Cole-Parmer instrument (Vernon Hills, IL), and 25 mL clear glass vials with caps were purchased from Fishersci (Hampton, NH).

**Instrumentation.** The Raman spectrometer used was from PerkinElmer (RamanStation 400F), equipped with a diode laser operating system at 785 nm with an average power of 100 mW (a relatively high power to increase signal intensity, Figure S1) at the sample and 100  $\mu$ m spot size. This RamanStation was equipped with the Raman Micro 300, which has a movable stage and a built-in camera monitoring the sample surface. The laser source was focused on the sample on the stage through a fiber optics cable connecting the RamanStation 400F to the RamanMicro 300. Usually, the 20× optical lens was employed in order to get better sample focus and Raman signal response. One piece of silicon wafer was employed to calibrate the Raman system on a daily basis, and the Raman signal intensity at 522 cm<sup>-1</sup> was monitored in order to see whether the instrument was functioning normally. In a typical Raman spectrometer measurement, the optical lens was adjusted to obtain the best image of the sample surface before the measurement was performed. The SERS measurement parameters used were as follows: laser wavelength, 785 nm; exposure time, 1 s; 4 exposures per measurement.

A Veeco multimode nanoscope III D atomic force microscope (AFM) was employed to obtain the surface morphology of the prepared AgNFs and monitor the changes of surface morphology during the cleaning and silanization procedures. A transmission electron microscope (TEM, Hitachi, H-7650) was employed to study the morphology of citrate-coated silver nanoparticles. A Malvern Zetasizer Nano-ZS (Westborough, MA) was employed to obtain the size and zeta potential of the nanoparticles synthesized in the laboratory. The average hydrodynamic diameters of the nanoparticles were obtained from the "Z-average" intensity peak as a function of size. UV—vis absorption spectra of AgNFs were obtained from a Cary 300 UV—vis spectrometer. All pH

measurements were carried out on a Fisher Scientific Accumet Research AR15 pH/mV/°C Meter.

Fabrication and Characterization of AgNFs. The fabrication process of AgNFs consisted of two major steps: synthesis of citrate-coated silver nanoparticles (AgNPs-Citrate)<sup>37</sup> and immobilization of the AgNPs-Citrate onto glass substrates.<sup>38</sup> AgNPs-Citrate was synthesized by reducing silver nitrate with sodium citrate. Briefly, all glassware was soaked in Aqua Regia (HCl/HNO<sub>3</sub> = 3:1, v/v) overnight, then rinsed with a large amount of tap water and DI water, and finally dried in an oven at 80 °C before use. Then a 250 mL round-bottom flask with 50 mL of  $1 \times 10^{-3}$  mol L<sup>-1</sup> silver nitrate was heated to boil in an oil bath under vigorous stirring with a condenser equipped to reflux. Sodium citrate solution (2 mL, 1% (w/v)) was added dropwise to the hot solution and kept boiling for 1 h to yield a greenish yellow AgNPs-Citrate colloidal suspension. Particle size and surface charge of the AgNPs-Citrate and pH of the colloidal suspension were obtained after the solution cooled down to room temperature.

For the process of immobilization of AgNPs onto glass substrates, all glass substrates (about  $1 \times 1 \text{ cm}^2$ ) were soaked in Aqua Regia solution overnight and then sonicated successively in concentrated NaOH solution (2 mol L<sup>-1</sup>) and HCl solution (2 mol L-1) for 2 h. These glass substrates were thoroughly rinsed with a large amount of tap water and DI water to wash away excess acid or base. Finally, these glass substrates were dried in an 80 °C oven prior to use. Then the AgNF was fabricated following a two-step procedure.<sup>38</sup> The first step was the silanization reaction on glass substrates surface to attach APTMS molecules catalyzed by a diluted acid.<sup>39</sup> APTMS solutions with different concentrations [0.5%, 1.0%, 2.5%, 5.0%, and 10.0% (v/v)] in anhydrous ethanol were first prepared. Then five pieces of glass substrates were soaked in a 25 mL glass vial containing 10 mL of APTMS solution and 100  $\mu$ L of 1 M HCl solution for 4 h on an orbital shaker (150 rpm). After the silanization reaction, the glass substrates were cleaned with anhydrous ethanol under sonication for 3 min and repeated four times in order to remove loosely attached APTMS molecules on the glass surface. These treated glass substrates were then dried by nitrogen and heated in an oven at 80 °C for 30 min before the next step. The second step was to immobilize AgNPs-Citrate onto the treated glass substrates. AgNPs-Citrate were immobilized by electrostatic interaction with the glass surface, since the amine groups were facing outward and positively charged in solution. The highaffinity interaction between silver nanoparticles and amine groups should further enhance the attachment. 38-40 Briefly, five pieces of glass substrates prepared from the first step were placed in a small weighing boat with no overlapping among the slides. Next, 5 mL of AgNPs solution was carefully transferred into a weighing boat, and the glass slides were submerged in the solution for different time periods (4, 8, and 24 h) on an orbital shaker (50 rpm). DI water was introduced to make up for the evaporation over time in order to prevent nanoparticles from aggregation. The resulting glass substrates were then cleaned with DI water three times, dried under N2 gas, and stored in a freezer prior to use.

The prepared AgNFs were examined for SERS signal enhancement using  $\mathrm{As^{III}}$  (1.33  $\times$  10<sup>-3</sup> mol L<sup>-1</sup> (100 ppm as arsenic atomic concentration) in DI water) as a model arsenical, and the fabrication process of AgNFs was optimized to obtain sufficient enhancement for arsenic SERS signals. The optimization was focused on the concentrations of APTMS

used in the silanization reaction and the immobilization times for AgNPs—Citrate on the silanized glass surfaces. The AgNFs prepared by the optimized method were characterized by AFM to obtain surface morphology and AgNF thickness.

SERS Fingerprint Signals of Arsenicals on the AgNFs. The typical fingerprint SERS signals of four commonly detected arsenicals including As<sup>III</sup>, As<sup>V</sup>, MMA<sup>V</sup>, and DMA<sup>V</sup> were measured individually in liquid droplets (0.1 mol L<sup>-1</sup> potassium phosphate buffer, pH = 7.5) and on dry stain after drying out the liquid droplet. To do so, stock solutions of arsenic compounds  $(13.3 \times 10^{-3} \text{ mol L}^{-1} \text{ or } 1000 \text{ ppm}$  as arsenic atomic concentration) were diluted to  $1.33 \times 10^{-3}$  mol L<sup>-1</sup> (100 ppm as arsenic atomic concentration) with 0.1 mol  $L^{-1}$  potassium phosphate buffer (pH = 7.5) as substock solutions. Typically, 2 µL of arsenic solution from substocks was dropped onto the AgNF, and SERS signals were collected randomly at the center region of the sessile droplet. After about 35 min of evaporation, the droplet was completely dry and a ring-shaped stain was formed on the AgNF due to the coffee ring effect. The SERS signals were collected at the edge region of the stain, where the analytes should be most concentrated.

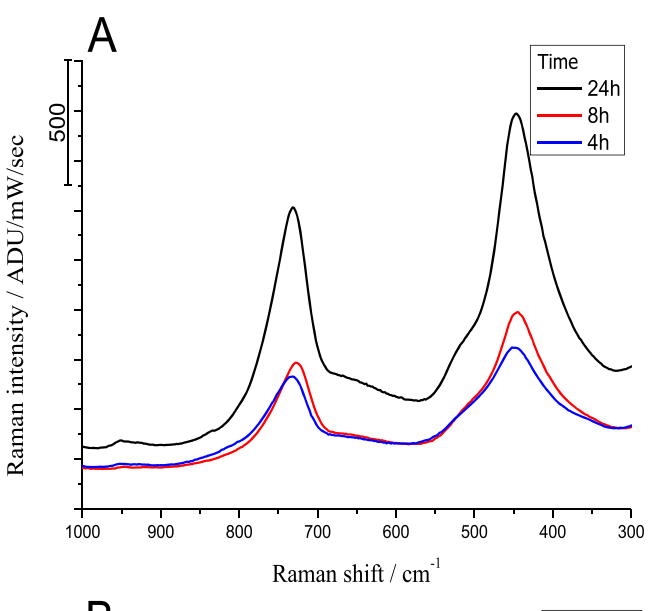
Arsenicals Speciation on the AgNFs. Arsenic speciation on AgNFs was investigated by sequential addition of individual arsenic standards, starting from AsV, followed by DMAV, MMAV, and AsIII to eventually have a mixture of the four arsenicals. In order to increase the separation, surfactant (0.05% of SDS) was added to the arsenic solutions with the purpose of extending the movement of the solvent on the surface. Arsenic standard solutions containing individual or mixed arsenicals of  $1.3 \times 10^{-3}$  mol L<sup>-1</sup> (100 ppm) for each species were prepared in 0.1 mol L<sup>-1</sup> phosphate buffer (pH = 7.5) with 0.05 wt % of SDS. One drop (2  $\mu$ L) of the solution was placed onto the AgNF surface, and the sessile droplet was allowed to dry on a flat bench under ambient conditions. While formation of only one ring-shaped stain occurs in a typical coffee ring phenomenon, two concentric ring-shaped stains were formed after drying the solution with SDS. Similar with the previous work of Brochard-Wyart et al., 34,35 the threephase contact line did not move during the evaporation of sessile droplets containing surfactants, but the liquid in the sessile droplet permeated into the peripheral region of the sessile droplet. There was a clear boundary between these two concentric rings, named here the inner ring and outer ring, respectively. The diameter of the inner and width of outer rings were measured in multiple experiments, and they ranged from 5.50 to 5.88 mm and from 3.45 to 3.90 mm, respectively, with relative standard deviations of 5-13% (Table S1 and Figure S2). SERS measurements on all coffee ring drop stains were typically carried out from the center all the way to the outer ring edge along the radius of the rings, and the sampling spots were performed with 100  $\mu$ m increments according to the on-screen meter and 10  $\mu m$  inside and outside the ring boundary as well.

## ■ RESULTS AND DISCUSSION

Optimization of Parameters for Fabrication and Characterization of AgNFs. Self-assembled metal colloid monolayer films have been widely used as SERS substrates. One method to prepare a stable nanofilm is to coat gold or silver colloid particles through chemical binding on a polymer surface with pendent functional groups, such as  $-NH_2$  or -SH. In this study, we first prepared AgNPs colloidal solutions and then modified glass slides with APTMS for anchoring the

AgNPs onto the surface to prepare AgNFs. The pH of AgNPs–Citrate colloidal solution was 9.0, and the surface of AgNPs was negatively charged with a zeta potential of -45.25 mV (Figure S3A). Because the p $K_a$  value of primary ammonium ( $-NH_3^+$ ) is greater than 10, APTMS was positively charged in the AgNPs colloidal solution.<sup>39</sup> Therefore, the positively charged surface can firmly bind with the negatively charged AgNPs to form stable AgNFs.<sup>39,40</sup>

We first optimized the soaking time of ATPMS-modified glass slides in AgNPs-Citrate solution (with 2.5% of APTMS) to get a sufficient SERS enhancement. There was a positive correlation between the length of immobilization time and the SERS signal intensity as shown in Figure 1A. The AgNF fabricated by 24 h of immobilization of AgNPs yielded the strongest signal response, and a higher signal was observed for



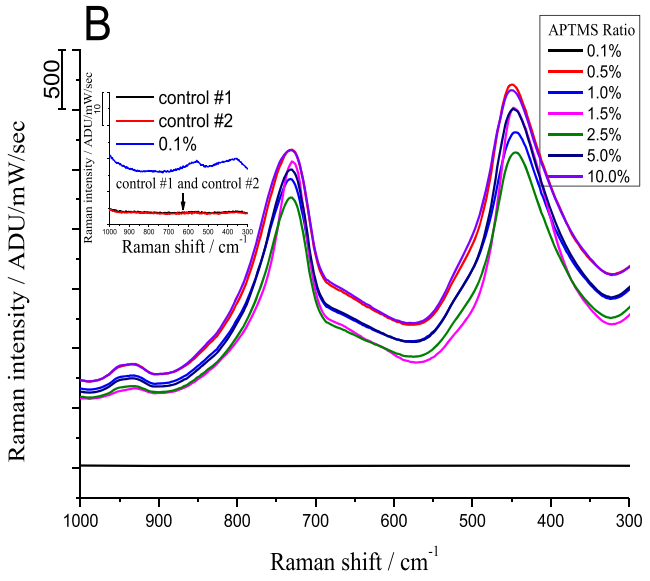
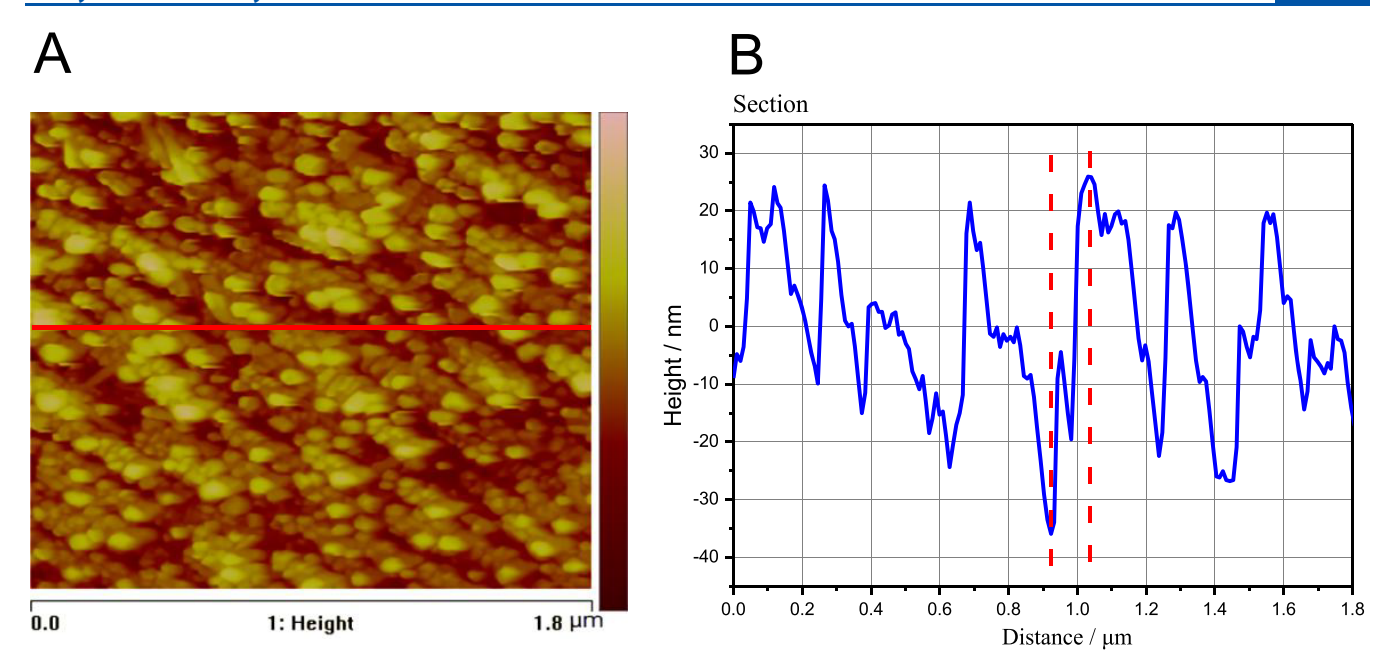


Figure 1. SERS signals of 2  $\mu$ L of 1.3  $\times$  10<sup>-3</sup> mol L<sup>-1</sup> (100 ppm) As<sup>III</sup> solution were obtained on different AgNFs for optimization of the AgNFs preparation method. (A) AgNFs were prepared by submerging the 2.5% (v/v) APTMS silanized glass slides in AgNPs solution for different times. (B) AgNFs were prepared from different concentrations of APTMS, including two controls. (Inset) control 1, bare glass slides; control 2, glass slide without salinization procedure.

8 h than 4 h. The time of immobilization was selected as 8 h in the later experiments for the sake of saving time and increasing signals. A further optimization on the immobilization time between 8 and 24 h might provide a better point for balancing experimental time and signal enhancement but was deemed not necessary at this stage for method development. We then examined the relationship between As<sup>III</sup> SERS signal intensity and the amount of APTMS used in silanization process (Figure 1B). No SERS signals were observed from the two control experiments, including the bare glass slide and the glass slide without APTMS treatment, and only hardly distinguishable signals were obtained by using 0.1% APTMS. These results indicated that the AgNF serves as a critical substrate for signal enhancement, and the silanization procedure is the prerequisite condition to fabrication of AgNF. The signal intensities when using 0.5-10.0% APTMS were similar, albeit varying slightly with minor baseline fluctuation. It is unclear why 2.5% APTMS yielded the lowest signals, while both lower (0.5-1.5%) and higher (5.0-10.0%) concentrations produced higher signal intensities. It would be understandable if all concentrations higher than 2.5% resulted in lower signal enhancement, as the excessive amount of APTMS might be greater than monolayer formation on the SERS substrate surface and cause AgNPs aggregation. Although 0.5% APTMS seemed to be sufficient for treatment of glass substrates, 1.0% APTMS was employed in the following experiments for arsenic detection for the convenience of preparation.

The AgNF prepared with the optimized method was characterized by AFM. The glass surface was coated thoroughly with AgNPs (bright dots shown in Figure 2A), although the arrangement was not well organized. An AFM cross-section of the sample is shown in Figure 2B. Ten random sections were selected in order to calculate the mean vertical distance in terms of the AgNF thickness, which was found to be  $48.7 \pm 6.7$  nm (n = 10). The size of AgNPs was about  $44.6 \pm 6.5$  nm (n = 9) according to the TEM imaging (Figure S15), similar to the z-average measurement results by Zetasizer, suggesting that a monolayer film was formed.

SERS Signals of Arsenicals on the AgNFs. From the typical fingerprint SERS signals of As<sup>III</sup>, As<sup>V</sup>, MMA<sup>V</sup>, and DMAV measured in droplet and dry stain, significant interference from the buffer was not found in the Raman shift range of 1000-300 cm<sup>-1</sup> (Figure S4). For each arsenical, similar wavenumbers of characteristic SERS signals were found between the droplet and the dry stain (Figure 3). For As<sup>III</sup> (Figure 3A), a strong vibrational band at 730 cm<sup>-1</sup> was observed in the droplet, resulting from the As-O stretch mode, 41 and this characteristic vibrational band of As-O appeared at the same position after the sessile droplet dried completely. The band at 440 cm<sup>-1</sup> in the droplet (shifted to 415 cm<sup>-1</sup> in dry stain) was not reported in the literature, and the vibrational mode of the arsenite molecule at 440 cm<sup>-1</sup> was tentatively interpreted as being the wagging of H-O bonds, with the assistance of computational chemistry (see Supporting Information for details, Figure S5). For As<sup>V</sup>, fingerprint signals at 792 and 782 cm<sup>-1</sup> were observed in the sessile droplet and on dry film, respectively, and these signals could be assigned to the As-O symmetric vibrations (Figure 3B).<sup>42</sup> The superposition stretch of  $\nu 2$  and  $\nu 5$  of the arsenate molecule was not distinguishable in this buffer solution, which usually appeared around 400 cm<sup>-1</sup>. <sup>42</sup> Similar SERS signal profiles were found for the two organoarsenicals. A vibrational band at 619 cm<sup>-1</sup> due to the As-C stretch and one broad vibrational band at 812



**Figure 2.** Typical surface morphology using (A) AFM depth imaging and (B) the cross-section profile for the prepared AgNF. Representative cross-section profile (Figure 2B) was obtained on the red line in Figure 2A. Vertical distance was the distance between the valley and the peak as the two dashed lines indicated.

cm<sup>-1</sup> from the vibrational band of As-O<sup>43</sup> were observed for MMA<sup>V</sup> (Figure 3C). For DMA<sup>V</sup>, the symmetric stretching of As-C appeared at 600 cm<sup>-1</sup> since DMA<sup>V</sup> has two As-C bonds, and the asymmetric As-O stretching was found at 830 cm<sup>-1</sup> (Figure 3D).<sup>16</sup> On the basis of the intensity of the characteristic signals on AgNFs, the strongest signal for each arsenical was selected as their fingerprint signal for speciation, and the wavenumbers of these signals were 730, 792, 619, and 600 cm<sup>-1</sup> for As<sup>III</sup>, As<sup>V</sup>, MMA<sup>V</sup>, and DMA<sup>V</sup>, respectively.

Experiments were repeated multiple times separately to evaluate the reproducibility of the SERS spectra and signal intensities on different sets of AgNFs (prepared from different batches of AgNPs but the same sizes), the size effects of AgNPs on the formation of coffee ring and SERS signal enhancement, and the variations of SERS signals with measuring times, with information provided in the Supporting Information. It was demonstrated that the SERS spectra and signal intensities on different sets of AgNFs of the same size were highly reproducible (Figures S6-S8). Although an increase in AgNP size from 50 to 70 nm did not change the SERS signal remarkably, a larger size of AgNPs (90 nm) could result in the decrease in SERS intensity, probably due to the decrease in the surface packing density of AgNPs on the film reproducibly (Figures S9). Measurements within 8 h after the coffee ring formation would generate reproducible SERS data (Figures S10–S13), but it would be desirable to perform SERS measurements immediately after the drop drying on the AgNFs for the sake of precaution.

While the characteristic wavenumbers were not significantly shifted, the signal intensities were found to be notably different in droplets and dry stains. Greater SERS enhancements on dry stains were observed for MMA<sup>V</sup> and DMA<sup>V</sup>. These organic arsenicals were negatively charged in the buffer; therefore, it was difficult for them to get close to the negatively charged AgNFs (surface zeta potential  $-48.21 \pm 1.40$  mV as determined by streaming potential measurements, see SI for additional experimental information) to generate strong SERS

signals in solution. Compared to solution droplets, stronger Raman signals were observed on dry stains because of the reduced distance to the AgNFs. The coffee ring effect also allows analytes in the droplet central area to travel to the edge with the solvent during the evaporation process, and the analytes can be concentrated in the drop stain area. Compared to the organic arsenicals, As and As III showed an opposite trend in which the SERS signals were decreased on the dry film compared to in solution, especially for As<sup>III</sup> with a significant signal decrease (Figure 3A). We speculated that this could be related to the As-AgNFs electrostatic interactions and the adsorption of arsenic species on AgNFs. For As<sup>III</sup>, it remained in the neutral form in the buffer solution with little electrostatic repulsion or attraction by the negatively charged AgNFs, but it could be adsorbed on the nanoparticle surface (probably to the citrate molecules) via van der Waals force. This adsorption would keep As<sup>III</sup> staying close enough to the surface to generate strong SERS signals in the solution. For AsV in the buffer solution, although it was negatively charged and thus repelled by the AgNF, the adsorption through van der Waals force would to some degree offset the electrostatic repulsion, thus retaining AsV close to the surface for SERS signal enhancement. Since As<sup>III</sup> was adsorbed on the AgNF (probably more strongly than AsV), it might not be able to move to the edge during the evaporation process and seemed to spread out in the stain area, causing the decrease in concentration at each spot. The appearance of a signal for As<sup>III</sup> at 730 cm<sup>-1</sup> throughout the dry stain spot from the central to the edge, when examining the movement of AsIII during drop evaporation, supported this notion (Figure 4A). In addition, the signal at 795 cm<sup>-1</sup> was observed from the middle to the edge area (particularly at the edge of the ring) in the SERS profile of As<sup>III</sup> in the dry stain, indicating possible formation of As and thus causing the decrease in As III signal. Such oxidation reaction was reported in a previous study, in which more than 70% As<sup>III</sup> was oxidized to As<sup>V</sup> in 1 mol L<sup>-1</sup> of ammonium hydroxide solution after a 90 min TLC separation

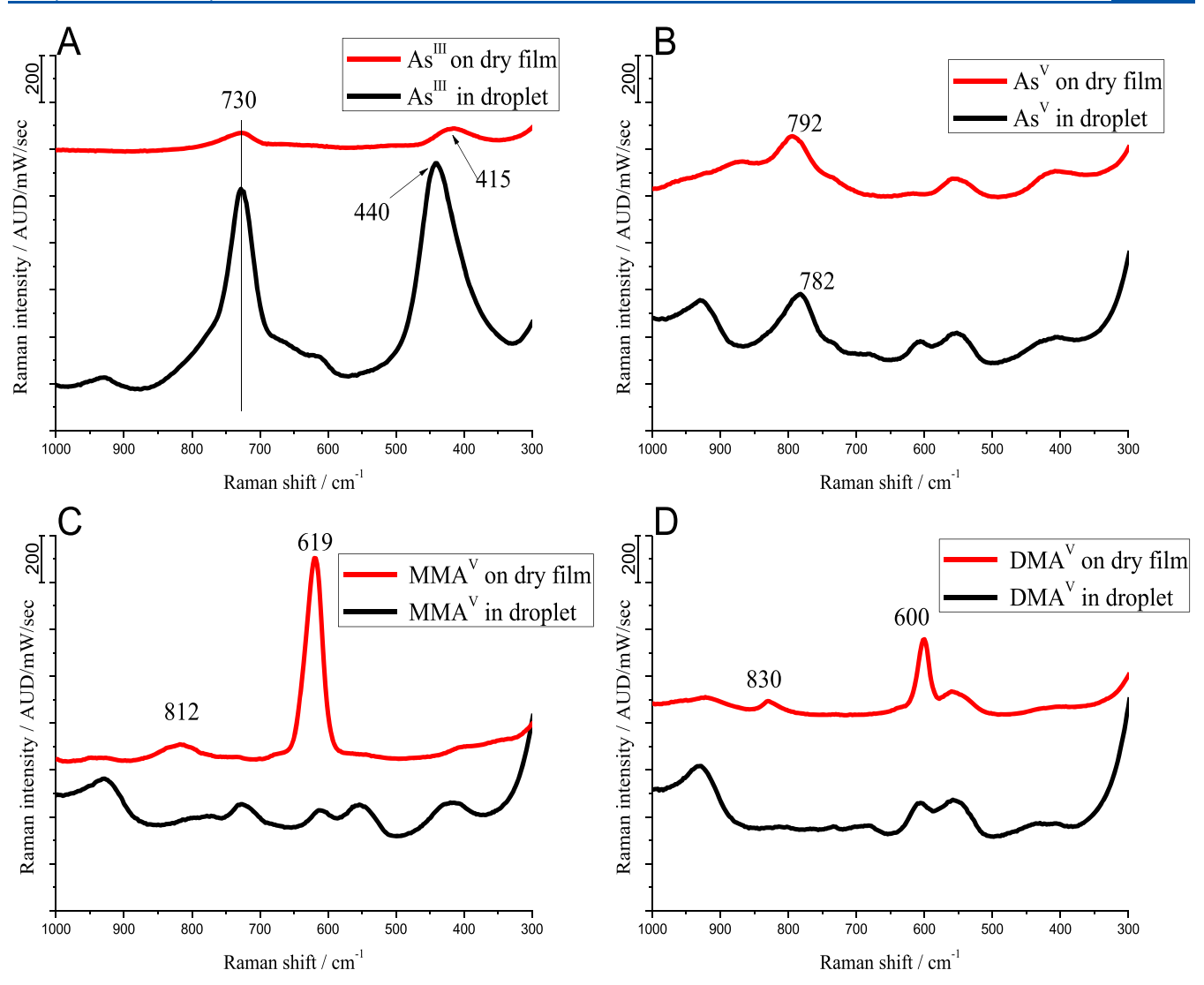


**Figure 3.** Typical SERS signal profiles of (A) As<sup>III</sup>, (B) As<sup>V</sup>, (C) MMA<sup>V</sup>, and (D) DMA<sup>V</sup> on the AgNFs. All signals in black curves were obtained at the center of the droplet containing 2  $\mu$ L of 1.3 × 10<sup>-3</sup> mol L<sup>-1</sup> (100 ppm) arsenic in 0.1 mol L<sup>-1</sup> potassium phosphate buffer (pH = 7.5) on AgNFs, and red curves represent signals obtained at the edge region after the sessile droplets evaporated.

on cellulose plate. He was suggested that the laser-excited surface plasmon resonance on the AgNPs played an important role in the oxidation reaction. The surface plasmon resonance can facilitate not only the activation of oxygen to form triplet oxygen molecules ( $^3O_2$ ) but also electron transfer from AgNPs to the  $^3O_2$  to create the anion of oxygen ( $^2O_2^-$ ). The  $^2O_2^-$  was then strongly adsorbed over the surface of AgNFs, and AgO $_2$  was formed under a high temperature locally raised by the laser. Therefore, the resulting AgO $_2$  could oxidize As to As on the surface. The appearance of As was then confirmed in a SERS profile obtained by measuring the drop stain of As along the radius (Figure 4B), where As at 783 cm was present in the outer ring area only.

The results of examining SERS signals of the four arsenic species indicated that these arsenicals exhibited distinct signal profiles with fair SERS enhancement on the AgNFs. It was also observed that the arsenic compounds traveled different distances with the solvent during the evaporation process and then deposited into different distribution patterns on the AgNFs. Taken together these results suggest that arsenic speciation could be potentially achieved by measurement of SERS signals along the radius of the ring stains.

Arsenic Speciation on the AgNFs. Although these four arsenicals showed different fingerprint vibrational bands, similarity of signal patterns from the two organoarsenicals caused a big problem for arsenic speciation analysis, according to our previous study by using colloidal suspension of AgNPs as a SERS substrate.<sup>24</sup> Nanofilms, as an alternative substrate, could offer a great advantage due to the coffee ring effect occurring during the evaporation of the droplet. In addition to preconcentration of the analytes, the coffee ring effect could facilitate the separation of arsenic species on the film due to the different interactions of arsenic with the substrate surface and the solvent. We thus used the AgNFs here for speciation of these four arsenicals, with the addition of 0.05% SDS to extend the movement of the solvent and enhance separation of arsenicals on the surface. The addition of SDS did not show interference to arsenic fingerprint signals (Figure S4) but lowered the surface tension of droplets and indeed increased the travel distance of the solution, resulting in the formation of two concentric rings that could be helpful for species

For As<sup>V</sup> alone, the strongest signal at 783 cm<sup>-1</sup> was found in the middle area of the outer ring and there was no obvious

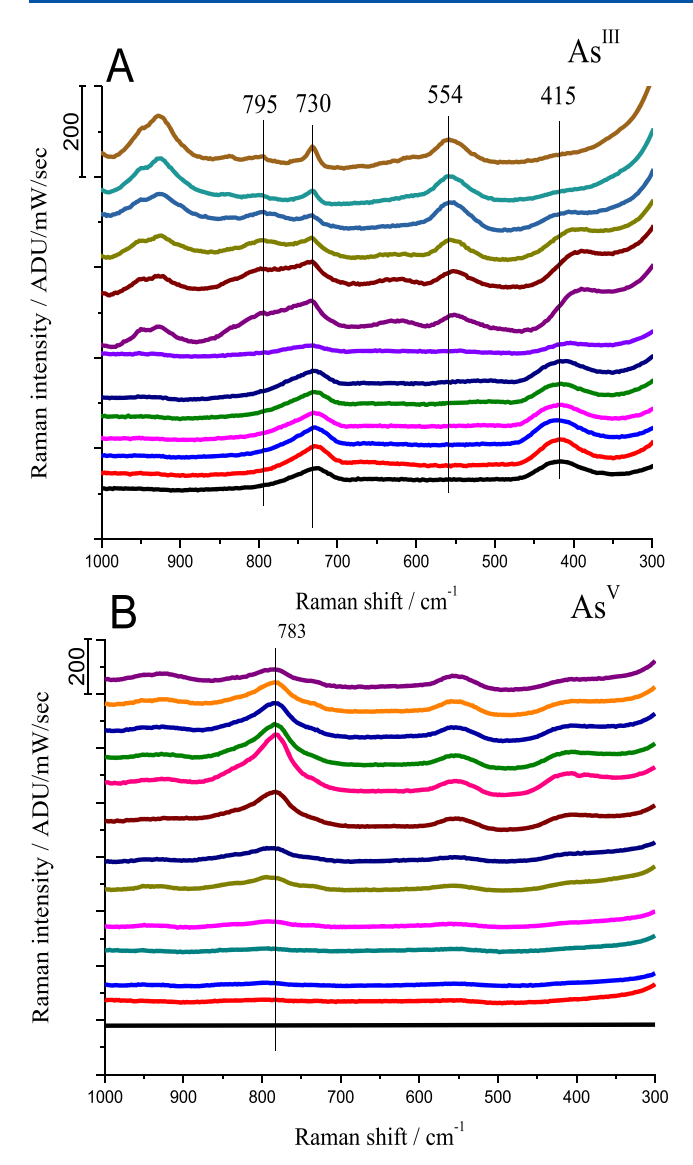


**Figure 4.** SERS signal profile of a drop stain after evaporation of 2  $\mu$ L of  $1.3 \times 10^{-3}$  mol L<sup>-1</sup> (100 ppm) (A) As<sup>III</sup> and (B) As<sup>V</sup> solution on the AgNF. Signals were collected along the radius of the drop stain from center to edge.

signal in the inner ring area (Figure 4B). For the mixture of As<sup>V</sup> and DMA<sup>V</sup>, the fingerprint signals of As<sup>V</sup> at 786 cm<sup>-1</sup> were still only in the outer ring area (Figure 5A) but the DMAV signals at 604 cm<sup>-1</sup> were observed in the inner ring, demonstrating that AsV and DMAV could be separated completely without any overlap. Figure 5B shows the speciation of adding MMAV to the mixture of AsV and DMA<sup>V</sup> on the AgNF. For As<sup>V</sup> and DMA<sup>V</sup>, their fingerprint signals, which were at 785 and 604 cm<sup>-1</sup>, respectively, appeared at the same region with that in Figure 5A. There was a new peak clearly appearing at 619 cm<sup>-1</sup> in the outer ring, resulting from the addition of MMAV. These results suggest that even if the fingerprint signals of MMAV and DMAV were close to each other, speciation of MMAV and DMAV could be accomplished on AgNF because of the physical separation of these two species achieved using the coffee ring effect. Finally, the SERS profile of the mixture of As<sup>III</sup>, As<sup>V</sup>, MMA<sup>V</sup>, and DMAV was measured with a shortened distance of each sampling spot from the center to the edge to avoid missing any

fingerprint signals. The characteristic peaks at 608 cm<sup>-1</sup>, assigned to DMAV, were found in most areas of the inner ring and consistently observed in the inner ring region until the boundary (Figure 5C). When the sampling spots moved into the outer ring area, the peak at 618 cm<sup>-1</sup> (see Figure S14 for its deconvolution and identification) appeared and remained unchanged in the entire outer ring, indicating the presence of MMA<sup>V</sup>. The fingerprint signal at 732 cm<sup>-1</sup> appearing throughout the outer ring area can be assigned to As<sup>III</sup>. Although the As<sup>III</sup> signals on the AgNFs were weak due possibly to the oxidation to AsV, the peaks were still clear and distinguishable. It is worth noting that the As<sup>III</sup> signals were not observed in the inner ring, different from the result for measuring As<sup>III</sup> alone (Figure 4A), probably due to the enhanced movement by the addition of SDS. The strongest As v signals at 778 cm<sup>-1</sup> were present in the middle of the outer ring, consistent with the results from the experiment for As<sup>V</sup>, MMA<sup>V</sup>, and DMA<sup>V</sup> (Figure 5B). These results indicated the successful speciation of As<sup>III</sup>, As<sup>V</sup>, MMA<sup>V</sup>, and DMA<sup>V</sup> on the AgNFs by combining the advantages of distinct fingerprint SERS signals and physical separation of arsenicals under the influence of coffee ring effect.

There was a significant difference between arsenic SERS profiles in the inner ring and the outer ring areas. The inner ring stain was formed by the coffee ring effect caused by an evaporation-driven capillary flow from the center of the droplet toward the contact line, while the outer ring stain was formed after adding a small amount of SDS containing buffer. The surfactant lowered the surface tension of the droplet, and consequently, the liquid could be slowly leaked out from the droplet because of capillary action caused by narrowly packed AgNPs surrounding the droplet. As a result, the arsenicals in a solution could move outward with the capillary flow to the edge of the droplet and then permeate into the periphery of the droplet with solvent. AgNFs provided a negatively charged surface to interact with the analytes, playing an important role in the physical separation of arsenicals. For example, the strongest MMA<sup>V</sup> signal appeared at the beginning of the outer ring, while DMAV appeared in the edge of the inner ring (Figure 5C), because  $MMA^V$  (pka = 3.6) bears more negative charges than DMA<sup>V</sup> (p $K_a = 6.2$ ) in the buffer (pH = 7.5).<sup>46</sup> Surfactant could also affect the migration of arsenicals during solvent evaporation. Because of the coffee ring effect, SDS near the contact line was concentrated and the surface tension near the drop edge decreased. The difference in surface tension resulted in a Marangoni flow toward the center to push the analytes backward. 47 Most of DMAV seemed to be trapped in the inner ring, possibly because the two methyl groups of DMAV had a high affinity to the hydrophobic chain of SDS, leading to the deposition of DMAV together with SDS in the inner ring area. On the contrary, MMAV has one methyl group and should have a weaker interaction with SDS, and thus, most of MMAV was found in the outer ring area. Another factor in play here is the eluting ability of solvent. The aqueous solution has a low eluting ability to less polar analytes such as DMAV (in comparison to MMAV)48 and thus limits its migration. Under the combined interactions with the surface, SDS, and the solvent, DMAV showed the shortest traveling distance.

# CONCLUSIONS

A novel method for arsenic speciation was explored by utilizing AgNFs as SERS substrates, combing the distinct fingerprint SERS signals of arsenicals and their physical separation caused

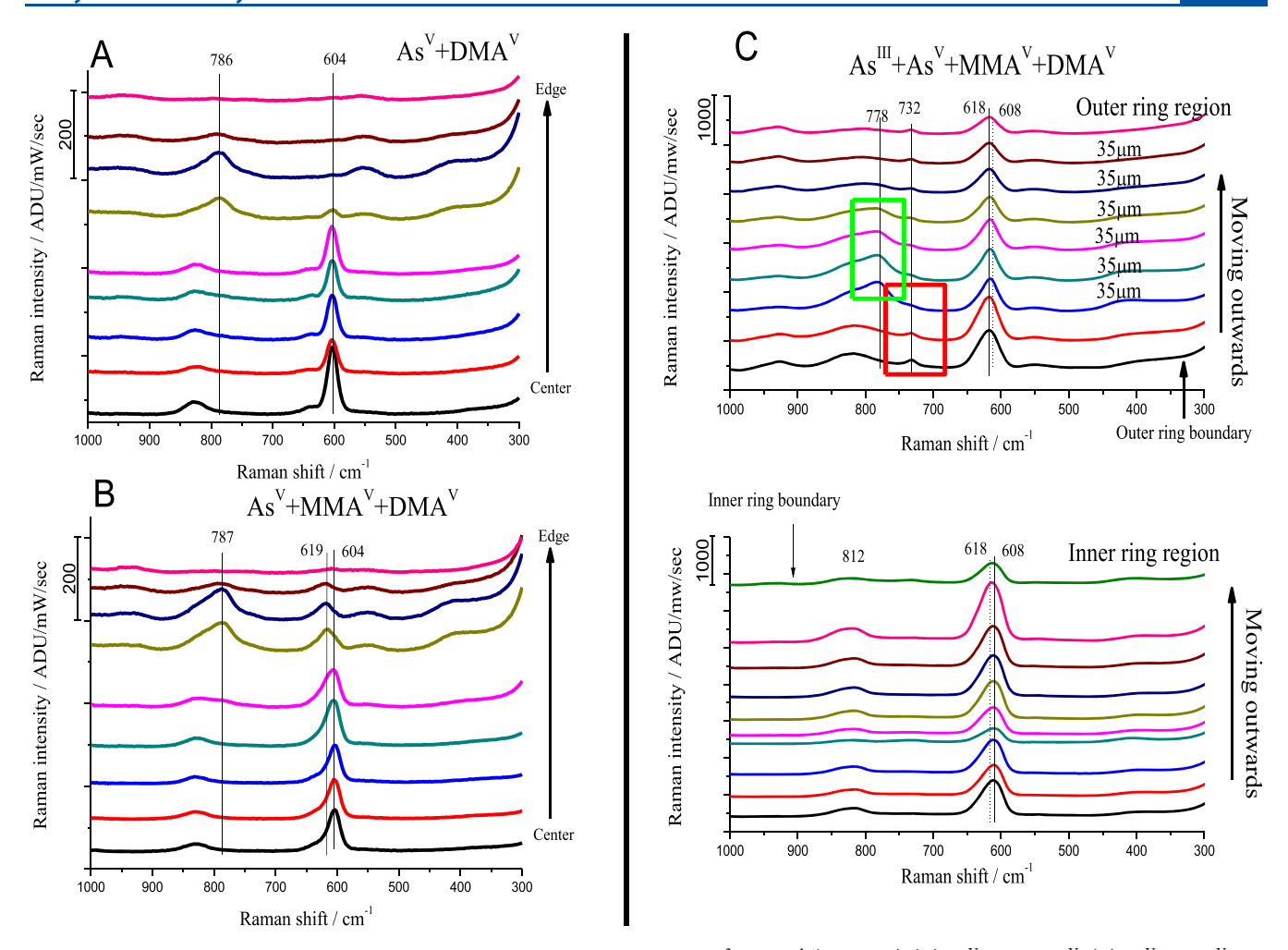


**Figure 5.** SERS signal profile of a drop stain after evaporation of 2  $\mu$ L of 1.3 × 10<sup>-3</sup> mol L<sup>-1</sup> (100 ppm) (A) As<sup>V</sup> and DMA<sup>V</sup>, (B) As<sup>V</sup>, MMA<sup>V</sup>, and DMA<sup>V</sup>, and (C) As<sup>V</sup>, MMA<sup>V</sup>, DMA<sup>V</sup>, and As<sup>III</sup> solution on a AgNF. Signals were collected along the radius of the drop stain from the center to the edge.

by the coffee ring effect on the AgNFs. In order to realize the possibility of using the coffee ring effect to separate small molecules, SDS as a surfactant was introduced, allowing varying travel distances for different arsenicals and thus successful speciation of As<sup>III</sup>, As<sup>V</sup>, MMA<sup>V</sup>, and DMA<sup>V</sup>. We demonstrated in this study the dual functions of AgNFs, as SERS substrates for signal enhancement and as a charged surface affecting analyte immigration. The capillary flow caused by the coffee ring effect also played a dual role, as it preconcentrated analytes into the ring edge area and meanwhile moved arsenicals to different distances on the AgNF surface. This is the very first study employing the coffee ring effect for arsenic speciation, and it does show the promising potential of the coffee ring effect for fast and in situ separation of small molecules. As the migration of analytes during evaporation is a complicated process controlled by various factors such as surface retention, capillary flow, and capillary action, future research will focus on understanding the role of these factors and further optimization of important factors for possible quantitative analysis of arsenic species.

# ASSOCIATED CONTENT

## S Supporting Information

The Supporting Information is available free of charge on the ACS Publications website at DOI: 10.1021/acs.analchem.9b00999.

Ancillary information for characterization of the AgNPs, background SERS signals, data reproducibility, additional peak deconvolution and identification, and SERS signal variations with time (PDF)

#### AUTHOR INFORMATION

# **Corresponding Author**

\*Tel: 305-348-6210. Fax: 305-348-3772. E-mail: cai@fiu.edu.

ORCID

Guangliang Liu: 0000-0003-4248-1167 Fengfu Fu: 0000-0002-8823-7672 Yong Cai: 0000-0002-2811-4638

# **Present Address**

Department of Biochemistry, Fraternal Order of Eagles Diabetes Research Center, Obesity Research and Education Initiative, University of Iowa Carver College of Medicine, 169 Newton Road, Iowa City, Iowa 52242, United States.

#### **Author Contributions**

\*M.Y. and V.L.: These authors contributed equally to this work.

#### **Notes**

The authors declare no competing financial interest.

## ACKNOWLEDGMENTS

The authors gratefully acknowledge the NSF program (ECS1710111) for the support of the work. We thank Dr. Abuzar Kabir in the Department of Chemistry and Biochemistry, FIU, for help during the fabrication of silver nanofilms and Prof. Wenzhi Li in the Department of Physics, FIU, for instrumental support in obtaining surface morphology of silver nanofilms. M.Y. acknowledges the Florida International University for financial support for dissertation research. We thank the anonymous reviewers whose comments have greatly improved this manuscript. This is contribution #908 from the Southeast Environmental Research Center in the Institute of Water & Environment at Florida International University.

# REFERENCES

- (1) Yehiayan, L.; Pattabiraman, M.; Kavallieratos, K.; Wang, X. T.; Boise, L. H.; Cai, Y. J. Anal. At. Spectrom. 2009, 24, 1397–1405.
- (2) Dufailly, V.; Nicolas, M.; Payot, J. R.; Poitevin, E. J. AOAC Int. **2011**, 94, 947–958.
- (3) Ammann, A. A. J. Chromatogr. A 2010, 1217, 2111-2116.
- (4) Yang, G.; Xu, J.; Zheng, J.; Xu, X.; Wang, W.; Xu, L.; Chen, G.; Fu, F. Talanta 2009, 78, 471–476.
- (5) Yehiayan, L.; Membreno, N.; Matulis, S.; Boise, L. H.; Cai, Y. *Anal. Chim. Acta* **2011**, *699*, 187–192.
- (6) Yang, G.-D.; Zheng, J.-P.; Huang, H.-X.; Qi, G.-M.; Xu, J.-H.; Fu, F.-F. Chin. J. Anal. Chem. **2009**, *37*, 532–536.
- (7) Kozak, L.; Niedzielski, P.; Szczuciński, W. Int. J. Environ. Anal. Chem. 2008, 88, 989–1003.
- (8) Gong, Z.; Lu, X.; Cullen, W. R.; Chris Le, X. J. Anal. At. Spectrom. 2001, 16, 1409-1413.
- (9) Kobayashi, Y.; Cui, X.; Hirano, S. Toxicology **2005**, 211, 115–123.
- (10) Conklin, S. D.; Fricke, M. W.; Creed, P. A.; Creed, J. T. *J. Anal. At. Spectrom.* **2008**, 23, 711–716.
- (11) Greaves, S. J.; Griffith, W. P. J. Raman Spectrosc. 1988, 19, 503-507.
- (12) Du, J.; Cui, J.; Jing, C. Chem. Commun. 2014, 50, 347-349.
- (13) Song, L.; Mao, K.; Zhou, X.; Hu, J. Talanta 2016, 146, 285–290.
- (14) Xu, Z.; Hao, J.; Li, F.; Meng, X. J. Colloid Interface Sci. 2010, 347, 90-95.
- (15) Gloria, D.; Moran, G.; Hibbert, D. B. In XXII International Conference on Raman Spectroscopy; Champion, P. M., Ziegler, L. D., Eds.; American Institute of Physics: Boston, MA, USA, 2010; pp 510–511.
- (16) Olavarría-Fullerton, J.; Wells, S.; Ortiz-Rivera, W.; Sepaniak, M. J.; De Jesus, M. A. Appl. Spectrosc. 2011, 65, 423–428.
- (17) Hao, J. M.; Han, M. J.; Xu, Z. H.; Li, J. W.; Meng, X. G. Nanoscale Res. Lett. **2011**, *6*, 263.
- (18) Xu, Z.; Jing, C.; Hao, J.; Christodoulatos, C.; Korfiatis, G. P.; Li, F.; Meng, X. *J. Phys. Chem. C* **2012**, *116*, 325–329.
- (19) Xu, Z.; Meng, X.; Zhang, Y.; Li, F. Colloids Surf., A 2016, 497, 117–125.
- (20) Li, J.; Chen, L.; Lou, T.; Wang, Y. ACS Appl. Mater. Interfaces 2011, 3, 3936–3941.
- (21) Ye, L.; Wen, G.; Dong, J.; Luo, Y.; Liu, Q.; Liang, A.; Jiang, Z. RSC Adv. **2014**, 4, 32960–32964.
- (22) Hao, J.; Han, M.-J.; Han, S.; Meng, X.; Su, T.-L.; Wang, Q. K. J. Environ. Sci. 2015, 36, 152–162.

- (23) Mulvihill, M.; Tao, A.; Benjauthrit, K.; Arnold, J.; Yang, P. Angew. Chem., Int. Ed. 2008, 47, 6456–6460.
- (24) Yang, M.; Matulis, S.; Boise, L. H.; McGoron, A. J.; Cai, Y. Anal. Bioanal. Chem. 2017, 409, 4683–4695.
- (25) Deegan, R. D.; Bakajin, O.; Dupont, T. F.; Huber, G.; Nagel, S. R.; Witten, T. A. *Nature* **1997**, 389, 827–829.
- (26) Kočišová, E.; Procházka, M.; Šípová, H. J. Raman Spectrosc. 2016, 47, 1394–1396.
- (27) Wang, W.; Yin, Y.; Tan, Z.; Liu, J. Nanoscale 2014, 6, 9588-9593.
- (28) Wong, T. S.; Chen, T. H.; Shen, X. Y.; Ho, C. M. Anal. Chem. **2011**, 83, 1871–1873.
- (29) Devlin, N. R.; Loehr, K.; Harris, M. T. AIChE J. 2015, 61, 3547–3556.
- (30) Li, D.; Qu, L.; Zhai, W.; Xue, J.; Fossey, J. S.; Long, Y. Environ. Sci. Technol. **2011**, 45, 4046–4052.
- (31) Zhu, Q.; Yu, X.; Wu, Z.; Lu, F.; Yuan, Y. Anal. Chim. Acta 2018, 1014, 64-70.
- (32) Zhu, Q.; Cao, Y.; Cao, Y.; Chai, Y.; Lu, F. Anal. Bioanal. Chem. 2014, 406, 1877–1884.
- (33) Ho, Y. C.; Lee, W. W. Y.; Bell, S. E. Analyst 2016, 141, 5152-5158.
- (34) Brochard-Wyart, F.; Fondecave, R.; Boudoussier, M. *Int. J. Eng. Sci.* **2000**, 38, 1033–1047.
- (35) Fondecave, R.; Wyart, F. B. Europhys. Lett. 1997, 37, 115-120.
- (36) Maher, W. A.; Foster, S.; Krikowa, F.; Duncan, E.; St John, A.; Hug, K.; Moreau, J. W. *Microchem. J.* **2013**, *111*, 82–90.
- (37) Lee, P.; Meisel, D. J. Phys. Chem. 1982, 86, 3391-3395.
- (38) Grabar, K. C.; Freeman, R. G.; Hommer, M. B.; Natan, M. J. Anal. Chem. 1995, 67, 735-743.
- (39) Bharathi, S.; Fishelson, N.; Lev, O. Langmuir 1999, 15, 1929–1937.
- (40) Aslan, K.; Holley, P.; Geddes, C. D. J. Mater. Chem. 2006, 16, 2846–2852.
- (41) Loehr, T. M.; Plane, R. A. Inorg. Chem. 1968, 7, 1708-1714.
- (42) Vansant, F. K.; Van Der Veken, B. J.; Desseyn, H. O. J. Mol. Struct. 1973, 15, 425-437.
- (43) Vansant, F.; Van der Veken, B.; Herman, M. J. Mol. Struct. 1976, 35, 191-200.
- (44) Stýblo, M.; Delnomdedieu, M.; Hughes, M. F.; Thomas, D. J. J. Chromatogr., Biomed. Appl. 1995, 668, 21–29.
- (45) Huang, Y.-F.; Zhang, M.; Zhao, L.-B.; Feng, J.-M.; Wu, D.-Y.; Ren, B.; Tian, Z.-Q. Angew. Chem., Int. Ed. 2014, 53, 2353-2357.
- (46) National Research Council Arsenic in Drinking Water; The National Academies Press: Washington, DC, 1999; p 330.
- (47) Still, T.; Yunker, P. J.; Yodh, A. G. Langmuir 2012, 28, 4984–
- (48) Xie, D.; Mattusch, J.; Wennrich, R. J. Sep. Sci. 2010, 33, 817–825.